



Computational Modeling of Mixed Solids for CO₂ Capture Sorbents

Yuhua Duan

**National Energy Technology Laboratory, United States Department of Energy
626 Cochrans Mill Road, Pittsburgh, Pennsylvania 15236, USA
Yuhua.duan@netl.doe.gov**

Prepared for Presentation at
American Institute of Chemical Engineers
2015 Spring Meeting
11th Global Congress on Process Safety
Austin, Texas
April 27-30, 2015

UNPUBLISHED

AIChE shall not be responsible for statements or opinions contained
in papers or printed in its publications

Computational Modeling of Mixed Solids for CO₂ Capture Sorbents

Yuhua Duan

National Energy Technology Laboratory, United States Department of Energy

626 Cochran's Mill Road, Pittsburgh, Pennsylvania 15236, USA

Yuhua.duan@netl.doe.gov

Keywords: CO₂ solid sorbents, *ab initio* thermodynamics, first-principles density functional theory, lattice phonon dynamics, computational screening

Abstract

Since current technologies for capturing CO₂ to fight global climate change are still too energy intensive, there is a critical need for development of new materials that can capture CO₂ reversibly with acceptable energy costs. Accordingly, solid sorbents have been proposed to be used for CO₂ capture applications through a reversible chemical transformation. By combining thermodynamic database mining with first principles density functional theory and phonon lattice dynamics calculations, a theoretical screening methodology to identify the most promising CO₂ sorbent candidates from the vast array of possible solid materials has been proposed and validated. The calculated thermodynamic properties of different classes of solid materials versus temperature and pressure changes were further used to evaluate the equilibrium properties for the CO₂ adsorption/desorption cycles. According to the requirements imposed by the pre- and post- combustion technologies and based on our calculated thermodynamic properties for the CO₂ capture reactions by the solids of interest, we were able to screen only those solid materials for which lower capture energy costs are expected at the desired pressure and temperature conditions. Only those selected CO₂ sorbent candidates were further considered for experimental validations. The *ab initio* thermodynamic technique has the advantage of identifying thermodynamic properties of CO₂ capture reactions without any experimental input beyond crystallographic structural information of the solid phases involved. Such methodology not only can be used to search for good candidates from existing database of solid materials, but also can provide some guidelines for synthesis new materials. In this presentation, we apply our screening methodology to mixing solid systems to adjust the turnover temperature to help on developing CO₂ capture Technologies.

1. Introduction

Nowadays, the burning of fossil fuels is still the main energy source for the world's economy. One consequence of the use of these fuels is the emission of huge quantities of CO₂ into the atmosphere creating environmental problems such as global climate warming.¹⁻⁵ In order to solve such problems, there is a need to reduce CO₂ emissions into atmosphere by capturing and sequestering CO₂.^{4,6,7} One approach to solve such environmental problems is to capture and sequester the CO₂. Current technologies for capturing CO₂ including solvent-based (amines) and CaO-based materials are still too energy intensive. Hence, there is critical need for development of new materials that can capture and release CO₂ reversibly with acceptable energy costs. In particular, solid oxide sorbent materials have been proposed for capturing CO₂ through a

reversible chemical transformation leading primarily to formation of carbonate products. Solid sorbents containing alkali and alkaline earth metals have been reported in several previous studies to be promising candidates for CO₂ sorbent applications due to their high CO₂ absorption capacity at moderate working temperatures.⁸⁻¹¹

During past few years we developed a theoretical methodology to identify promising solid sorbent candidates for CO₂ capture by combining thermodynamic database searching with *ab initio* thermodynamics obtained based on first-principles density functional theory (DFT) and lattice phonon dynamics.^{8-10, 12-16} As shown in Fig.1, the primary outcome of our screening scheme is a list of promising CO₂ sorbents with optimal energy usage.

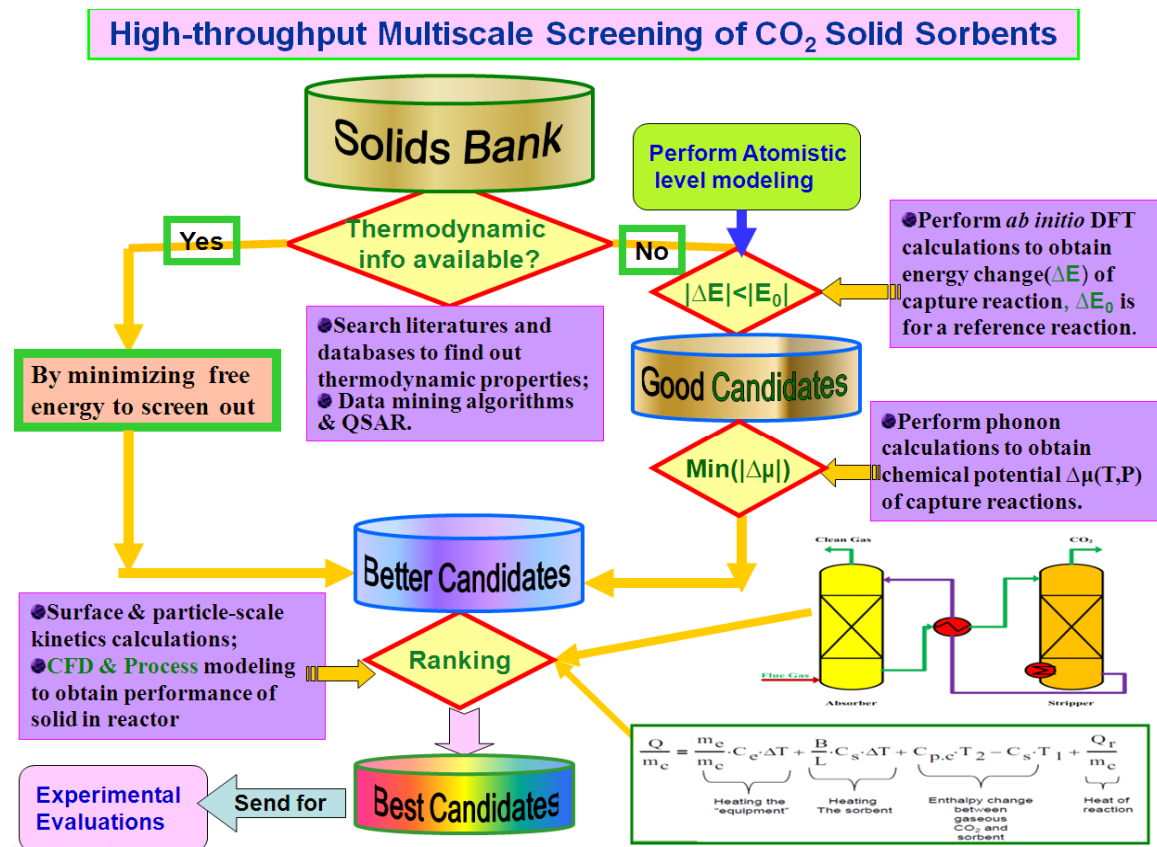


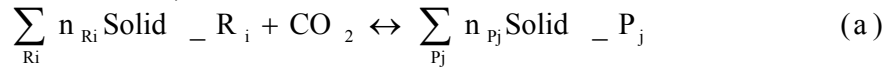
Fig. 1. Schematic of our screening methodology.

At a given CO₂ pressure, the turnover temperature (T_t) of an individual solid capture CO₂ reaction is fixed. Such T_t may be outside the operating temperature range (ΔT_o) for a particular capture technology. In order to adjust T_t to fit the practical ΔT_o, in this study, we demonstrate that by mixing different types of solids it's possible to shift T_t to the range of practical operating conditions.

2. Calculation Methods for Mixed Solid Sorbents

The complete description of the computational methodology together with relevant applications can be found in our previous publications.^{8-10, 12-19} The CO₂ capture reactions of

solids can be expressed generically in the form (for convenient description, we normalized the reaction to 1 mole of CO_2)

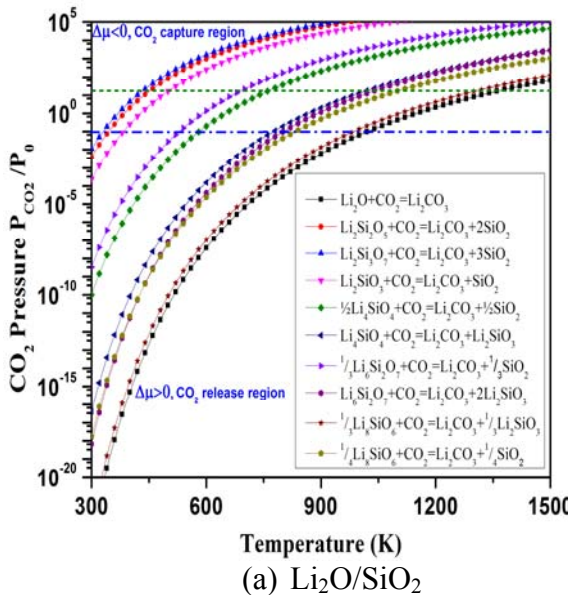


where n_{R_i} , n_{P_j} are the numbers of moles of reactants (R_i) and products (P_j) involved in the capture reactions. We treat the gas phase CO_2 as an ideal gas. By assuming that the difference between the chemical potentials ($\Delta\mu^0$) of the solid phases of reactants (R_i) and products (P_j) can be approximated by the difference in their total energies (ΔE^{DFT}), obtained directly from DFT calculations, and the vibrational free energy of the phonons and by ignoring the PV contribution terms for solids, the variation of the chemical potential ($\Delta\mu$) for reaction (a) with temperature and pressure can be written as^{8-10, 12-19}

$$\Delta\mu(T, P) = \Delta\mu^0(T) - RT \ln \frac{P_{\text{CO}_2}}{P_0} \quad (1)$$

where

$$\Delta\mu^0(T) \approx \Delta E^{\text{DFT}} + \Delta E_{\text{ZP}} + \Delta F^{\text{PH}}(T) - G_{\text{CO}_2}^0(T) \quad (2)$$



(a) $\text{Li}_2\text{O}/\text{SiO}_2$

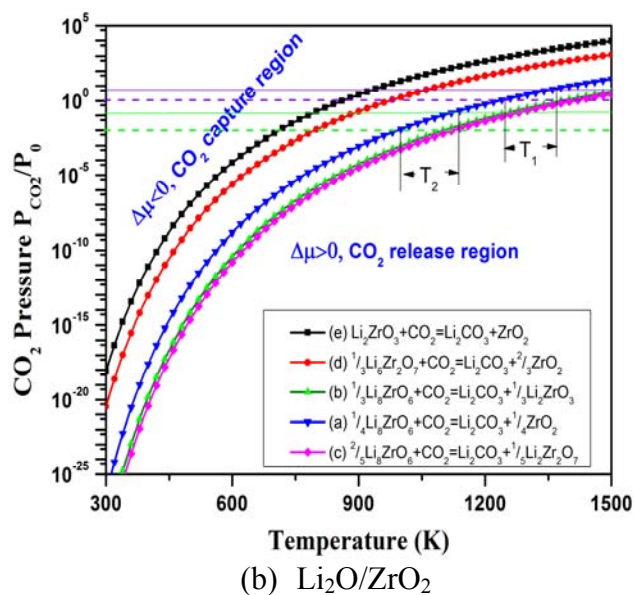


Fig. 2. Contour plots of the calculated chemical potential ($\Delta\mu$) versus temperature and the CO_2 pressure (P plotted in logarithmic scale) for the CO_2 capture reactions. Only $\Delta\mu=0$ curve is shown explicitly. For each reaction, above its $\Delta\mu=0$ curve, their $\Delta\mu<0$, which means the sorbents absorb CO_2 and the reaction goes forward, whereas below the $\Delta\mu=0$ curve, their $\Delta\mu>0$, which indicates CO_2 start to be released and reaction goes backward with regeneration of the sorbents.

Here, ΔE^{DFT} is the DFT energy difference between the reactants and products of the reaction (a), ΔE_{ZP} is the zero point energy difference between the reactants and products and can be obtained directly from phonon calculations. ΔF^{PH} is the phonon free energy change excluding zero-point energy (which is already counted into the ΔE_{ZP} term) between the solids of products and reactants. P_{CO_2} is the partial pressure of CO_2 in the gas phase and P_0 is the standard state reference pressure taken to be 1 bar. The heat of reaction ($\Delta H^{\text{cal}}(T)$) can be evaluated through the following equation

$$\Delta H^{\text{cal}}(T) = \Delta\mu^0(T) + T[\Delta S_{\text{PH}}(T) - S_{\text{CO}_2}(T)] \quad (3)$$

where $\Delta S_{\text{PH}}(T)$ is the difference of entropies between product solids and reactant solids. The free energy of CO_2 ($G^0_{\text{CO}_2}$) can be obtained from standard statistical mechanics,^{9, 10, 16} and its entropy (S_{CO_2}) can be found in the empirical thermodynamic databases.²⁰

3. Results and Discussions

For a given CO_2 capture process, its optimal working conditions (CO_2 pressures of pre- and after-capture, absorption/desorption temperature range (ΔT_o), *etc.*) were fixed. However, at a given CO_2 pressure, the turnover temperature (T_t) of an individual solid capture CO_2 reaction is fixed. Such T_t may be outside the operating temperature range ΔT_o for a particular capture technology. In order to adjust T_t to fit the practical working through reversible chemical transformations ΔT_o , we have demonstrated that by mixing different types of solids it's possible to shift T_t to the practical operating ΔT_o range.^{8, 21, 22} Generally, when we mix two solids *A* and *B* to form a new sorbent *C*, the turnover temperature of the newly resulted system (T_C) is located between those of *A* and *B* (T_A , T_B). Here it was assumed that *A* is a strong CO_2 sorbent while *B* is a weak CO_2 sorbent and $T_A > T_B$. Also, we assumed that the desired operating temperature T_o is between T_A and T_B ($T_A > T_o > T_B$). Depending on the properties of *A* and *B*, we have typically three scenarios to synthesize the mixing sorbent *C*:

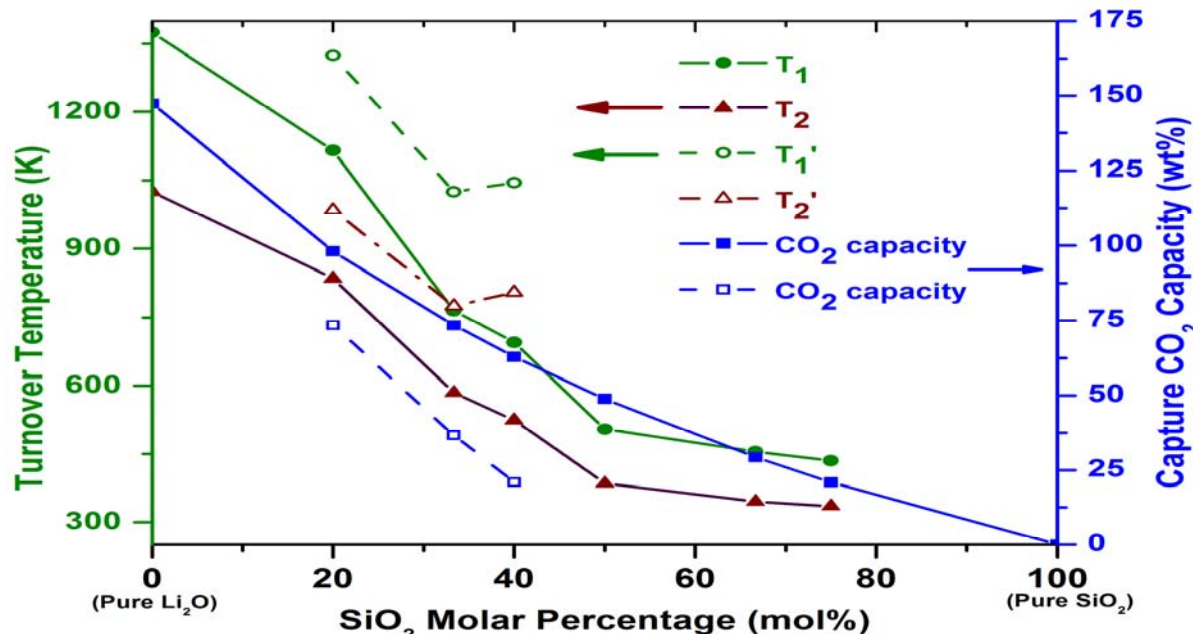


Fig. 3 The dependence of the turnover temperatures defined in the text and of CO_2 capture capacity on molar percentage of SiO_2 in the silicates for which calculations are reported here. T_1 and T_1' are the turnover temperatures under pre-combustion conditions with CO_2 partial pressure at 20 bars, while T_2 and T_2' are the turnover temperatures under post-combustion conditions with CO_2 partial pressure at 0.1 bar. The solid lines indicate to convert lithium silicates to SiO_2 and Li_2CO_3 (T_1 , T_2). For those Li_2O -rich lithium silicates (Li_8SiO_6 , Li_4SiO_4 , $\text{Li}_6\text{Si}_2\text{O}_7$) capturing CO_2 , the data shown in dash lines indicate convert them to Li_2SiO_3 and Li_2CO_3 (T_1' , T_2'). The corresponding CO_2 capture capacities are plotted with open blue squares.

3.1. $T_A \gg T_B$ and the A component is the key part to capture CO_2 .

An example of this case is represented by Li_2O . This is a very strong CO_2 sorbent which forms Li_2CO_3 . However, its regeneration from Li_2CO_3 only can occur at very high temperature (T_A). In order to move its T_A to lower temperatures, one can mix some weak CO_2 sorbents (such as SiO_2 , ZrO_2). Fig. 2 shows the relationship of chemical potential, P_{CO_2} , and T of the CO_2 capture reactions by the mixed $\text{Li}_2\text{O}/\text{SiO}_2$ and $\text{Li}_2\text{O}/\text{ZrO}_2$ solids with different mixing ratios. Fig. 3 shows the turnover temperature and the CO_2 capture capacity of $\text{Li}_2\text{O}/\text{SiO}_2$ mixture versus the ratio of $\text{Li}_2\text{O}/\text{SiO}_2$.^{8-10, 12, 18, 21, 23, 24}

From Figs. 2 and 3, one can see that after mixing Li_2O and SiO_2 (or ZrO_2) with different $\text{Li}_2\text{O}/\text{SiO}_2$ (or $\text{Li}_2\text{O}/\text{ZrO}_2$) ratios, the T_C of the newly formed C compound (silicate or zirconate) is lower than T_A of pure Li_2O and could be close to the ΔT_o range to fit the practical needs.

3.2 $T_A \gg T_B$ and B component is the key part to capture CO_2

In this case, since T_B is lower than T_o , by mixing A into B will increase the turnover temperature T_C of the C solid to values closer to T_o . For example, pure MgO has a very high theoretical CO_2 capture capacity. However, its turnover temperature (250 °C) is lower than the required temperature range of $300\text{--}470$ °C used in warm gas clean up technology and its practical CO_2 capacity is very low, and therefore, it cannot be used directly as a CO_2 sorbent in this technology.²⁵⁻²⁷ As shown in Fig. 4, by mixing alkali metal oxides M_2O ($\text{M}=\text{Na, K, Cs, Ca}$) or carbonates (M_2CO_3) into MgO , the corresponding newly formed mixing systems have higher turnover temperatures making them useful as CO_2 sorbents through the reaction $\text{MgO} + \text{CO}_2 + \text{M}_2\text{CO}_3 = \text{M}_2\text{Mg}(\text{CO}_3)_2$.^{25, 28}

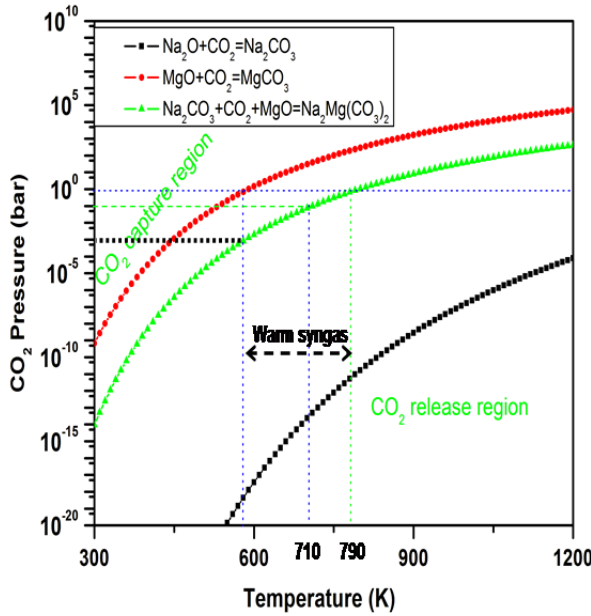
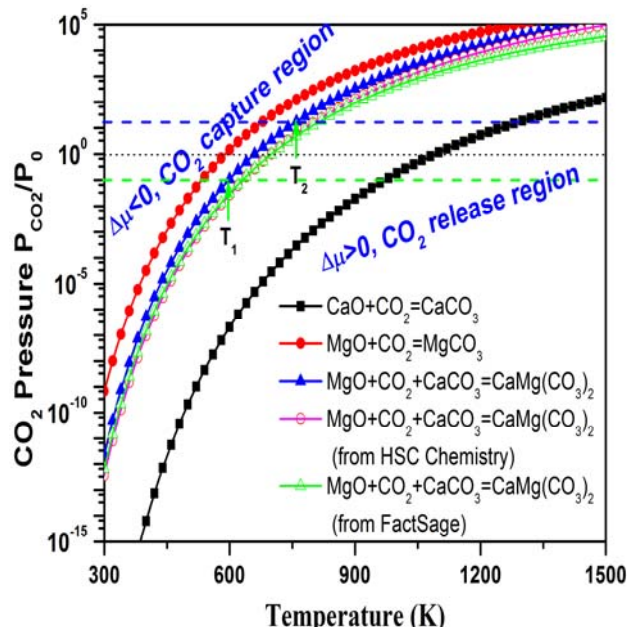
(a) $\text{MgO}/\text{Na}_2\text{CO}_3$ (Na_2O)(b) MgO/CaCO_3 (CaO)

Fig. 4. Plots of the calculated chemical potentials versus CO_2 pressures and temperatures for the CO_2 capture reaction by MgO to form double salts.

3.3 T_A and T_B are close to each other and both A and B are active for CO_2 capture

In this case, both A and B components are active to capture CO_2 , and the CO_2 capacity of the mixture is the summation of those of A and B . As we know another potential advantage of mixing solids is to increase the surface area of the solids in order to have faster reaction rates. Such a mixing scenario doesn't show too much advantage in shifting the capture temperature, but may enhance the kinetics of the capture process and eventually make the mixtures more efficient. Although there is no such report in literature, we think such an attempt is worthwhile and are working on several doped systems. Figure 5 shows a case of Na-/K- doped Li_2ZrO_3 capture CO_2 through the following reaction (b):²⁹

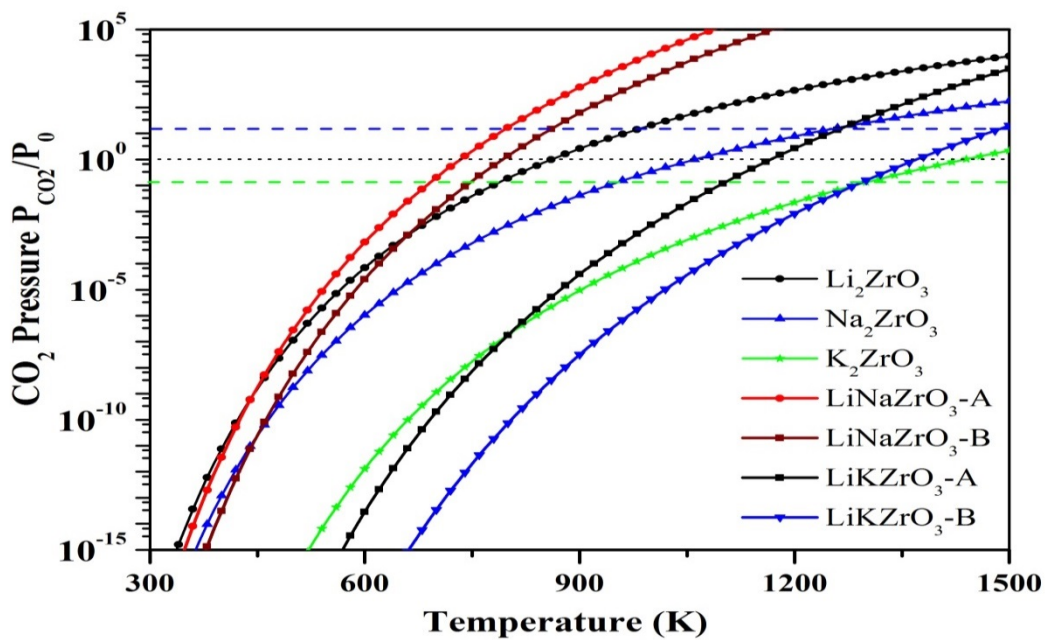


Fig. 5. The contour plotting of calculated chemical potentials versus CO_2 pressures and temperatures of the CO_2 capture reactions by LiMzrO_3 and M_2ZrO_3 . Y-axis plotted in logarithm scale. Only the $\Delta\mu=0$ curve is shown explicitly. For each reaction, above its $\Delta\mu=0$ curve, their $\Delta\mu<0$, which means the solids absorb CO_2 and the reaction goes forward, whereas below the $\Delta\mu=0$ curve, their $\Delta\mu>0$, which means the CO_2 start to release and the reaction goes backward to regenerate the sorbents.

All of the reactions are thermodynamically favorable for CO_2 sorption over a quite wide range of temperatures and reduced CO_2 pressures. But a well performing CO_2 solid sorbent should not only easily absorb CO_2 in the first half cycle but also easily release CO_2 from the product (M_2CO_3 and ZrO_2 for example) in the second half cycle. Table 1 shows the calculated thermodynamical properties and turnover temperatures of LiMzrO_3 capture CO_2 reaction (b).

From Fig.5 and Table 1, one can see that they are not good sorbents for capturing CO_2 for pre-combustion technology. However, they could be used for high-temperature post-combustion CO_2 capture with $T_2=685\text{ K}$, 745 K for LiNaZrO_3 (phases _A and _B) and $T_2=1095\text{ K}$, 1285 K for LiKZrO_3 (phases _A and _B) respectively. When compared to Li_2ZrO_3 , the K substituted system LiKZrO_3 does not decrease the turnover temperature of the CO_2 capture reaction. In other words,

although the LiKZrO_3 has a stronger driving force to capture CO_2 , with improved CO_2 capture capability when compared to Li_2ZrO_3 , its regeneration only can happen at higher temperature. Therefore, LiKZrO_3 is not a good CO_2 sorbent, since it requires more energy to regenerate. In contrast, the Na-substituted sorbent system LiNaZrO_3 does have a more compatible turn over temperature, making it a possible good candidate as a CO_2 sorbent. Such conclusions are in good agreement with experimental findings.³⁰⁻³²

In summary, from the calculated thermodynamic properties of LiMzrO_3 reacting with CO_2 , we found that the CO_2 sorbent performance of LiNaZrO_3 is better than that of Li_2ZrO_3 , but the performance of LiKZrO_3 is much worse since its regeneration temperature is higher. Therefore, the Na doped Li_2ZrO_3 , LiNaZrO_3 , is a better CO_2 sorbent for post-combustion capture technology. Our calculated thermodynamic results showed that the K doped Li_2ZrO_3 , LiKZrO_3 , didn't gain any improvements over Li_2ZrO_3 on its overall CO_2 capture performance.

Table 1. The weight percentage of CO_2 capture, the calculated energy change ΔE^{DFT} , the zero-point energy changes ΔE^{ZP} and the thermodynamic properties (ΔH , ΔG) of the CO_2 capture reactions. (unit: kJ/mol). The turnover temperatures (T_1 and T_2) of the reactions of CO_2 capture by solids under the conditions of pre-combustion ($P_{\text{CO}_2}=20$ bar) and post-combustion ($P_{\text{CO}_2}=0.1$ bar) are also listed.

reaction	absorbing CO_2 Wt%	ΔE^{DFT}	ΔE^{ZP}	ΔH ($T=300\text{K}$)	ΔG ($T=300\text{K}$)	Turnover T (K)	
						T_1	T_2
$\text{Li}_2\text{ZrO}_3+\text{CO}_2 \leftrightarrow \text{Li}_2\text{CO}_3+\text{ZrO}_2^{\text{a}}$	28.75	-146.648	11.311	-158.562	-103.845	1000	780
$\text{LiNaZrO}_3\text{A}+\text{CO}_2 \leftrightarrow \frac{1}{2}(\text{Li}_2\text{CO}_3+\text{Na}_2\text{CO}_3)+\text{ZrO}_2$	26.01	-152.936	7.069	-176.666	-110.892	805	685
$\text{LiNaZrO}_3\text{B}+\text{CO}_2 \leftrightarrow \frac{1}{2}(\text{Li}_2\text{CO}_3+\text{Na}_2\text{CO}_3)+\text{ZrO}_2$	26.01	-167.872	6.934	-191.526	-126.477	865	745
$\text{LiKZrO}_3\text{A}+\text{CO}_2 \leftrightarrow \frac{1}{2}(\text{Li}_2\text{CO}_3+\text{K}_2\text{CO}_3)+\text{ZrO}_2$	23.75	-264.115	6.006	-287.513	-225.611	1275	1095
$\text{LiKZrO}_3\text{B}+\text{CO}_2 \leftrightarrow \frac{1}{2}(\text{Li}_2\text{CO}_3+\text{K}_2\text{CO}_3)+\text{ZrO}_2$	23.75	-311.604	7.080	-332.612	-272.410	hT ^b	1285
$\text{Na}_2\text{ZrO}_3+\text{CO}_2 \leftrightarrow \text{Na}_2\text{CO}_3+\text{ZrO}_2^{\text{a}}$	23.76	-140.862	2.236	-158.327	-114.121	1275	925
$\text{K}_2\text{ZrO}_3+\text{CO}_2 \leftrightarrow \text{K}_2\text{CO}_3+\text{ZrO}_2^{\text{a}}$	20.24	-223.158	5.813	-238.490	-187.884	hT ^b	1285

^a from Refs.^{18, 23, 24}.

^b hT means the temperature is higher than our temperature range (1500K)

With similar approach, we have investigated the electronic structural and phonon properties of $\text{Na}_{2-\alpha}\text{M}_\alpha\text{ZrO}_3$ ($\text{M}=\text{Li, K}$, $\alpha=0, 0.5, 1.0, 1.5, 2.0$) by density functional theory and first-principles determination of phonon dynamics.³³ The thermodynamic properties of CO_2 absorption/desorption in these materials were analyzed. The obtained results are presented in Fig.6 and Table 2.

Based on the calculated relationships among the chemical potential change, CO_2 pressure and temperature for CO_2 capture reactions by $\text{Na}_{2-\alpha}\text{M}_\alpha\text{ZrO}_3$ and thermogravimetric analysis experimental measurements, compared to pure Na_2ZrO_3 , the Li- and K-doped mixtures $\text{Na}_{2-\alpha}\text{M}_\alpha\text{ZrO}_3$ have lower turnover temperatures (T_t) and higher CO_2 capacities. The calculated results show that the shift in T_t depends not only on the doping element, but also depends on the doping level. The Li-doped systems have larger T_t decreases than the K-doped systems. When increasing the Li-doping level α , the T_t of corresponding mixture $\text{Na}_{2-\alpha}\text{Li}_\alpha\text{ZrO}_3$ decreases further to a low temperature range. However in the case of K-doped systems $\text{Na}_{2-\alpha}\text{K}_\alpha\text{ZrO}_3$, although

initial doping of K into Na_2ZrO_3 can shift its T_t to lower temperature range, further increasing the K-doping level α results in an increase in T_t . Therefore, compared to K-doing, lithium inclusion into Na_2ZrO_3 structure has a larger influence on the CO_2 capture performance.

Table 2. The weight percentage of CO_2 capture, the ratios of $\text{Na}_2\text{O}:M_2\text{O}:\text{ZrO}_2$ ($M=\text{Li, K}$), the calculated energy change ΔE^{DFT} , the zero-point energy changes ΔE^{ZP} and the thermodynamic properties (ΔH , ΔG) of the CO_2 capture reactions. (unit: kJ/mol). The turnover temperatures (T_1 and T_2) of the reactions of CO_2 capture by solids under the conditions of pre-combustion ($P_{\text{CO}_2}=20$ bar) and post-combustion ($P_{\text{CO}_2}=0.1$ bar) are also listed.³³

reaction	absorbing CO_2 wt%	$\text{Na}_2\text{O}:M_2\text{O}:\text{ZrO}_2$ ratio	ΔE^{DFT}	ΔE^{ZP}	ΔH ($T=300\text{K}$)	ΔG ($T=300\text{K}$)	Turnover T (K)	
							T_1	T_2
$\text{Na}_2\text{ZrO}_3+\text{CO}_2 \leftrightarrow \text{Na}_2\text{CO}_3+\text{ZrO}_2$ ^a	23.76	1:0:1	-140.862	2.236	-158.327	-114.121	1275	925
$\text{Na}_{1.5}\text{Li}_{0.5}\text{ZrO}_3\text{-B}+\text{CO}_2 \leftrightarrow \frac{3}{4}\text{Na}_2\text{CO}_3+\frac{1}{4}\text{Li}_2\text{CO}_3+\text{ZrO}_2$	24.83	$\frac{3}{4}:\frac{1}{4}:1$	-170.881	4.667	-242.090	-159.144	805	715
$\text{Na}_{1.0}\text{Li}_{1.0}\text{ZrO}_3\text{-B}+\text{CO}_2 \leftrightarrow \frac{1}{2}\text{Na}_2\text{CO}_3+\frac{1}{2}\text{Li}_2\text{CO}_3+\text{ZrO}_2$	26.01	$\frac{1}{2}:\frac{1}{2}:1$	-157.839	6.480	-228.381	-142.555	745	675
$\text{Na}_{0.5}\text{Li}_{1.5}\text{ZrO}_3\text{-A}+\text{CO}_2 \leftrightarrow \frac{1}{4}\text{Na}_2\text{CO}_3+\frac{3}{4}\text{Li}_2\text{CO}_3+\text{ZrO}_2$	27.31	$\frac{1}{4}:\frac{3}{4}:1$	-169.827	9.652	-237.765	-146.230	735	665
$\text{Na}_{1.5}\text{K}_{0.5}\text{ZrO}_3\text{-A}+\text{CO}_2 \leftrightarrow \frac{3}{4}\text{Na}_2\text{CO}_3+\frac{1}{4}\text{K}_2\text{CO}_3+\text{ZrO}_2$	22.77	$\frac{3}{4}:\frac{1}{4}:1$	-210.081	2.486	-281.253	-199.996	915	825
$\text{Na}_{1.0}\text{K}_{1.0}\text{ZrO}_3\text{-B}+\text{CO}_2 \leftrightarrow \frac{1}{2}\text{Na}_2\text{CO}_3+\frac{1}{2}\text{K}_2\text{CO}_3+\text{ZrO}_2$	21.86	$\frac{1}{2}:\frac{1}{2}:1$	-245.436	2.058	-316.736	-236.789	1015	915
$\text{Na}_{0.5}\text{K}_{1.5}\text{ZrO}_3\text{-B}+\text{CO}_2 \leftrightarrow \frac{1}{4}\text{Na}_2\text{CO}_3+\frac{3}{4}\text{K}_2\text{CO}_3+\text{ZrO}_2$	21.02	$\frac{1}{4}:\frac{3}{4}:1$	-278.147	1.519	-349.077	-272.038	1125	1015
$\text{Li}_2\text{ZrO}_3+\text{CO}_2 \leftrightarrow \text{Li}_2\text{CO}_3+\text{ZrO}_2$ ^b	28.75	0:1:1	-146.648	11.311	-158.562	-103.845	1000	780
$\text{K}_2\text{ZrO}_3+\text{CO}_2 \leftrightarrow \text{K}_2\text{CO}_3+\text{ZrO}_2$ ^a	20.24	0:1:1	-223.158	5.813	-238.490	-187.884	hT ^c	1285

^a From Ref.²⁴.

^b From Ref.¹⁸

^c hT means the temperature is higher than 1500K

All these results may be of great interest in the development of specific CO_2 capture applications. As it has been shown, the $\text{Na}_{2-\alpha}\text{Li}_\alpha\text{ZrO}_3$ and $\text{Na}_{2-\alpha}\text{K}_\alpha\text{ZrO}_3$ compositions can produce modifications in the CO_2 capture temperatures, which may be used in the design of a specific composition depending on the temperature range that industry requires. Our work has identified that the capture of CO_2 in zirconate materials is not simply a matter of substitutional element, but also the doping level. This insight will need to be considered during future sorbent development. We have also demonstrated that computational methods can be used to accurately predict aspects of CO_2 capture and have the potential to drive future work by identifying the most promising candidate materials.

4. Conclusions

The obtained results showed that by changing the mixing ratio of solid *A* and solid *B* to form mixed solid *C* it's possible to shift the turnover T_t of the newly formed solid *C* to fit the practical CO_2 capture technologies. When mixing SiO_2 or ZrO_2 into the strong Li_2O sorbent, one can

obtain a series of lithium silicates (or zirconates) with T_t lower than that of pure Li_2O . By mixing oxides (Na_2O , K_2O , CaO) or their corresponding carbonates into MgO , the obtained mixtures exhibit different thermodynamic behaviors and their T_t are higher than that of pure MgO . Such results can be used to provide insights for designing new CO_2 sorbents. Therefore, although one single material taken in isolation might not be an optimal CO_2 sorbent to fit the particular needs to operate at specific temperature and pressure conditions, by mixing or doping two or more materials to form a new material, our results showed that it is possible to synthesize new CO_2 sorbent formulations which can fit the industrial needs. Our results also show that computational modeling can play a decisive role for identifying materials with optimal performance.

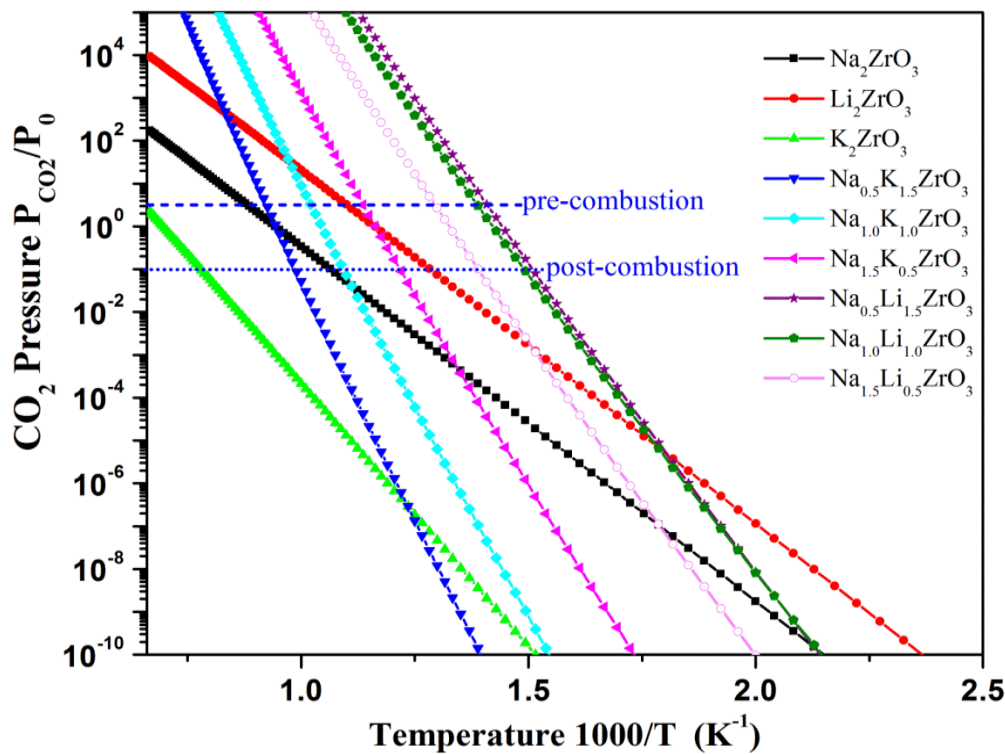


Fig. 6. The contour plotting of calculated chemical potential changes versus CO_2 pressures and temperatures of the reactions for $\text{Na}_{2-\alpha}\text{M}_\alpha\text{ZrO}_3$ ($\text{M}=\text{Li, K}$, $\alpha=0.5, 1.0, 1.5$) capture CO_2 . The typical CO_2 pressure for pre- and post-combustions are specified in blue lines.³³

Acknowledgement

The author thanks Drs. D. C. Sorescu, D. Luebke, H. W. Pennline, B. Y. Li, H. Pfeiffer, J. K. Johnson, B. Zhang, K. Zhang, D. King, K. Parlinski for their kind help and collaborations.

References

¹ D. Aaron, and C. Tsouris, Separation Science and Technology **40**, 321 (2005).

² C. M. White, B. R. Strazisar, E. J. Granite, J. S. Hoffman, and H. W. Pennline, J Air Waste Manag Assoc **53**, 645 (2003).

³ R. S. Haszeldine, Science **325**, 1647 (2009).

⁴ B. Y. Li, Y. Duan, D. Luebke, and B. Morreale, Applied Energy **102**, 1439 (2013).

⁵ M. R. Allen, D. J. Frame, C. Huntingford, C. D. Jones, J. A. Lowe, M. Meinshausen, and N. Meinshausen, Nature **458**, 1163 (2009).

⁶ H. Pfeiffer, and P. Bosch, Chemistry of Materials **17**, 1704 (2005).

⁷ E. Ochoa-Fernandez, H. K. Rusten, H. A. Jakobsen, M. Ronning, A. Holmen, and D. Chen, Catalysis Today **106**, 41 (2005).

⁸ Y. Duan, D. Luebke, and H. W. Pennline, International Journal of Clean Coal and Energy **1**, 1 (2012).

⁹ Y. Duan, and D. C. Sorescu, Phys Rev B **79**, 014301 (2009).

¹⁰ Y. Duan, and D. C. Sorescu, J Chem Phys **133**, 074508 (2010).

¹¹ Y. Duan, in *Proceedings of 7th~13th Ann. Conf. on Carbon Capture, Sequestration & Utilization* Pittsburgh, 2008-2014).

¹² Y. Duan, and K. Parlinski, Phys Rev B **84**, 104113 (2011).

¹³ Y. Duan, B. Zhang, D. C. Sorescu, and J. K. Johnson, J. Solid State Chem. **184**, 304 (2011).

¹⁴ Y. Duan, D. R. Luebke, H. W. Pennline, B. Y. Li, M. J. Janik, and J. W. Halley, Journal of Physical Chemistry C **116**, 14461 (2012).

¹⁵ Y. Duan, B. Zhang, D. C. Sorescu, J. K. Johnson, E. H. Majzoub, and D. R. Luebke, Journal of Physics-Condensed Matter **24**, 325501 (2012).

¹⁶ B. Zhang, Y. Duan, and J. K. Johnson, J Chem Phys **136**, 064516 (2012).

¹⁷ Y. Duan, Phys. Rev. B **77**, 045332 (2008).

¹⁸ Y. Duan, J Renew Sustain Ener **3**, 013102 (2011).

¹⁹ Y. Duan, J Renew Sustain Ener **4**, 013109 (2012).

²⁰ M. W. J. Chase, J. Phys. Chem. Ref. Data, **Monograph 9**, 1 (1998).

²¹ Y. Duan, Physical Chemistry Chemical Physics **15**, 9752 (2013).

²² Y. Duan, H. Pfeiffer, B. Li, I. C. Romero-Ibarra, D. C. Sorescu, D. R. Luebke, and J. W. Halley, Physical Chemistry Chemical Physics **15**, 13538 (2013).

²³ Y. Duan, H. Pfeiffer, B. Y. Li, I. C. Romero-Ibarra, D. C. Sorescu, D. R. Luebke, and J. W. Halley, Physical Chemistry Chemical Physics **15**, 13538 (2013).

²⁴ Y. Duan, J Renew Sustain Ener **4**, 013109 (2012).

²⁵ K. L. Zhang, X. H. S. Li, Y. Duan, D. L. King, P. Singh, and L. Y. Li, International Journal of Greenhouse Gas Control **12**, 351 (2013).

²⁶ K. L. Zhang, X. H. S. Li, W. Z. Li, A. Rohatgi, Y. Duan, P. Singh, L. Y. Li, and D. L. King, Advanced Materials Interfaces **1**, 1400030 (2014).

²⁷ J. L. Chi, L. F. Zhao, B. Wang, Z. Li, Y. H. Xiao, and Y. Duan, International Journal of Hydrogen Energy **39**, 6479 (2014).

²⁸ Y. Duan, K. Zhang, X. S. Li, D. L. King, B. Li, L. Zhao, and Y. Xiao, Aerosol and Air Quality Research **14**, 470 (2014).

²⁹ Y. Duan, ScienceJet **3**, 56 (2014).

³⁰ M. Y. Veliz-Enriquez, G. Gonzalez, and H. Pfeiffer, J Solid State Chem **180**, 2485 (2007).

³¹ H. Pfeiffer, E. Lima, and P. Bosch, Chemistry of Materials **18**, 2642 (2006).

³² H. Pfeiffer, C. Vazquez, V. H. Lara, and P. Bosch, Chemistry of Materials **19**, 922 (2007).

³³ Y. Duan, J. Lekse, X. F. Wang, B. Y. Li, B. Alcantar-Vazquez, H. Pfeiffer, and J. W. Halley, Physical Review Applied, accepted (2015).